



Magma-driven hydraulic fracturing and infiltration of fluids into the damaged host rock, an example from Dronning Maud Land, Antarctica

Ane K. Engvik^{a,*}, Andreas Bertram^b, Jörg F. Kalthoff^b, Bernhard Stöckhert^c, Håkon Austrheim^d,
Synnøve Elvevold^e

^a*Institutt for Geologi og Bergteknikk, Norges Teknisk-naturvitenskaplige Universitet, N-7491 Trondheim, Norway*

^b*Institut für Mechanik, Ruhr-Universität Bochum, D-44801 Bochum, Germany*

^c*Institut für Geologie, Mineralogie und Geophysik, Ruhr-Universität Bochum, D-44801 Bochum, Germany*

^d*PGP and Institutt for Geofag, Universitetet i Oslo, N-0316 Oslo, Norway*

^e*Norsk Polarinstitutt, N-9296 Tromsø, Norway*

Received 21 April 2004; received in revised form 15 November 2004; accepted 25 January 2005

Abstract

Excellent outcrops in Dronning Maud Land, Antarctica, provide unique insight into the mode and extent of fluid infiltration into metamorphic and plutonic rocks in the middle crust. The fluids are liberated from pegmatitic veins and give rise to alteration halos. In the alteration halos, the conspicuous change in colour is correlated with (1) hydration mineral reactions, and (2) high density of microcracks in quartz and feldspar exceeding that observed in the unaltered host rock by an order of magnitude. The field relations indicate that the veins originated as melt-driven hydraulic fractures, sealed by pegmatite and aplite crystallising from volatile-rich melts, with the alteration halo being the wake of the process zone formed at the tip of the propagating fractures. It is proposed that (1) the size of the alteration zone and the width of the vein are correlated, resulting in higher values of both these quantities for cracks propagating at higher velocities and consequently higher crack propagation toughnesses; (2) the damage zone is characterised by a transient state of high permeability which was short-lived due to rapid healing and sealing of microcracks; (3) the infiltration and retrogression of the high-grade rocks can be considered as a quasi-instantaneous process on geologic time scales with a duration of hours to weeks.

© 2005 Published by Elsevier Ltd.

Keywords: Alteration halo; Antarctica; Damage zone; Fluid infiltration; Hydraulic fracture; Process zone

1. Introduction

Pegmatite veins are supposed to form from hydraulic fractures driven by the excess pressure of intruding hydrous melts (e.g. Brisbin, 1986). For tensile cracks to form by hydraulic fracturing, the fluid pressure must exceed the magnitude of the least principal stress by the tensile strength of the rock (e.g. Secor, 1965; Shaw, 1980) or, in fracture mechanics terminology, exceed the fracture toughness of

the rock. Upon cooling and crystallisation, the portion of volatiles in the pegmatitic melt that is not incorporated into minerals is liberated as a fluid phase (Burnham, 1979). Transport of this fluid phase away from the crystallising magma is governed by the porosity and permeability of the host rock of the pegmatite vein.

Metamorphic and magmatic rocks in central Dronning Maud Land, East Antarctica, provide an outstanding insight into these phenomena due to the excellent quality of the exposures. In this area, pegmatitic veins were emplaced in high-grade metamorphic rocks and the fluids liberated from crystallising pegmatitic melt infiltrated the host rock on both sides of the central vein causing alteration. The extent of the infiltrated zones is conspicuous owing to the marked change of the rock colour from dark brown to light. This reveals a characteristic width of the alteration halo and a sharp boundary. Similar alteration zones around veins were described by Segall and Pollard (1983), Segall (1984a,b),

* Corresponding author. Tel.: +47 73 594804, fax: +47 73 594814

E-mail addresses: ane.engvik@geo.ntnu.no (A.K. Engvik), andreas.bertram@ruhr-uni-bochum.de (A. Bertram), joerg.f.kalthoff@ruhr-uni-bochum.de (J.F. Kalthoff), bernhard.stoekchert@ruhr-uni-bochum.de (B. Stöckhert), hakon.austrheim@geo.uio.no (H. Austrheim), elvevold@npolar.no (S. Elvevold).

Austrheim (1990) and Kostenko et al. (2002), for example. In the present paper, the basic geometric properties of the alteration halos flanking the pegmatitic veins in central Dronning Maud Land are described. Microscopic evidence for crack-controlled fluid infiltration controlling the extent of the alteration halos is presented. Alternative concepts for the origin of the damage zone flanking the pegmatite veins are discussed. Based on mechanical considerations, it is proposed that the damage zone that gave rise to the conspicuous alteration halo represents the wake of the advancing crack tip process zone of the hydraulic fracture, which developed into the pegmatite vein. The width of the light alteration zones hence reflects the radius of the process zone at the tip of the main fracture. Finally, it is suspected that the entire alteration process took place during a short period, rapidly halted by healing and sealing of the microcracks in the wake.

2. Geological setting and petrography of unaltered rocks

The mountain range of Dronning Maud Land, East Antarctica, was a part of Gondwana formed in late Neoproterozoic to early Paleozoic times (Jacobs et al., 1998; Fitzsimons, 2000). In Dronning Maud Land, Mesoproterozoic (ca. 1.1–1.0 Ga) rocks were intruded by voluminous intrusions and underwent granulite facies metamorphism and deformation during the Pan-African event (Elworthy, 1982; Ohta et al., 1990; Moyes, 1993; Mikhalsky et al., 1997; Jacobs et al., 1998). Mühlig-Hofmannfjella and Filchnerfjella consist of a series of granitoid intrusives, which are emplaced in granulite and upper amphibolite facies metamorphic host rocks (Ohta, 1999). In the area of 5–8°E three principal rock complexes of banded gneisses, charnockite and quartz syenite are distinguished (Fig. 1). The present study focuses on samples collected from three localities representing each of the different lithologies.

2.1. Banded gneisses

Banded gneisses include brown orthopyroxene-bearing gneiss, leucocratic gneiss, metapelite and garnet amphibolite. The gneisses have experienced granulite facies metamorphism and widespread anatexis. Peak metamorphic temperatures reached $>850\text{ }^{\circ}\text{C}$ at intermediate pressure, followed by a stage of near-isothermal decompression (Engvik and Elvevold, 2004). Granulite facies metamorphism in central Dronning Maud Land is dated as 590–515 Ma (Mikhalsky et al., 1997; Jacobs et al., 1998).

The migmatitic garnet–orthopyroxene gneiss of Kubusfjellet (locality 1) reveals a variable grain size on the sample scale, being characteristic for the different layers defining the foliation. The granoblastic matrix is made up of anhedral quartz and feldspar grains. The feldspars comprise plagioclase, orthoclase, perthite, and minor antiperthite. Myrmekite is common. Biotite flakes show a preferred orientation and are concentrated in thin layers together with orthopyroxene. Garnet is evenly distributed throughout the rock. Apatite, monazite, zircon, and ilmenite are accessory minerals.

2.2. Charnockite

The charnockite complex comprises massive, coarse-grained granite with igneous textures and granitic gneiss with well-developed banding and foliation. All gradations between preserved magmatic and gneissic textures are observed, all varieties revealing granulite facies mineral assemblages with orthopyroxene and biotite. The unfoliated granite commonly displays a weak preferred orientation of the euhedral tabular perthite megacrystals and locally diffuse dark bands enriched by orthopyroxene and biotite.

Reddish brown orthopyroxene-bearing charnockite of Svarthamaren (locality 2) displays a heterogranular texture and a fine- to medium grain size. Feldspars and quartz dominate the charnockite with minor myrmekite. The feldspars comprising perthite and plagioclase commonly

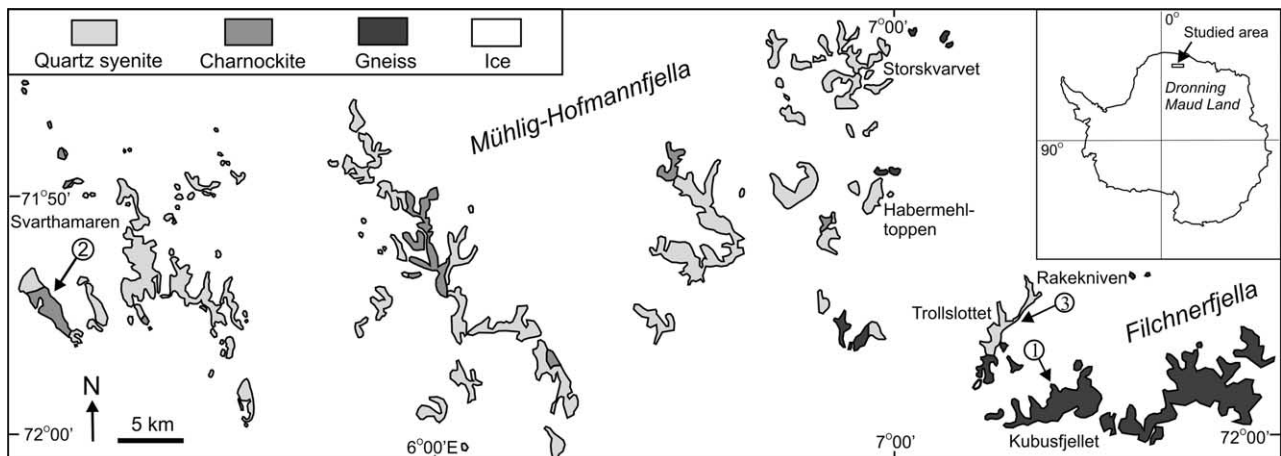


Fig. 1. Geological map of Mühlig-Hofmann and Filchnerfjella, Dronning Maud Land, Antarctica. The sample locations 1–3 are marked by encircled numbers.

occur as euhedral crystals. Biotite flakes are randomly oriented. Minor ferrosillite and hastingsite appear as anhedral grains. Apatite, zircon, monazite, ilmenite, hematite and Fe-oxides occur as accessory phases.

2.3. Quartz syenite

Massive, dark coloured quartz syenite is the major rock type in the study area. The intrusions belong to a large magmatic complex extending between 6 and 13°E. Brown quartz syenite of Trollslottet (locality 3) is coarse-grained to pegmatitic, and contains megacrystals of mesoperthitic K-feldspar. Perthite is the predominant mineral, accompanied by quartz, plagioclase, myrmekite, biotite and hastingsite. Minor orthopyroxene is associated with grunerite, biotite and hastingsite with fine-grained plagioclase and quartz. Apatite, ilmenite, zircon, allanite and hematite are accessory minerals. The field relations show that the quartz syenites intruded the banded gneisses and charnockite and represent a late stage in the intrusive history. The quartz syenite of Trollslottet is dated to 521 ± 4 Ma by U–Pb-geochronology on zircon (Paulsson, 2003).

3. Discordant pegmatite and aplite veins

The three rock types in the investigated area are characterised by a dark brown or reddish brown weathering colour. They are frequently cut by discordant conspicuous light bands, as shown in Fig. 2. The centre of the light bands is invariably constituted by a pegmatitic or aplitic vein with a thickness ranging from a few mm to about 15 cm (Fig. 2a–d). This indicates that the light zones originated as alteration halos around the veins. The marked change in macroscopic colour is correlated with a change in mineral assemblage and microstructure, as described below. The phenomenon is observed along the mountain range of Mühlig-Hofmannfjella and Filchnerfjella over a minimum length of 150 km, and has also been reported from areas further to the east (Markl and Piazzolo, 1998).

The veins in the centre of the alteration halos are composed of granitoid rocks referred to as aplite or pegmatite depending on grain size. The mineral assemblage in the veins indicates formation from a hydrous melt with a granitic composition, for which the solidus temperature is typically about 650–700 °C at a pressure of about 0.3 GPa (e.g. Merrill et al., 1970; Cox et al., 1979; Huang and Wyllie, 1981). The aplites and pegmatites are primarily composed of feldspar, quartz, biotite, locally green amphibole and accessory apatite, titanite, zircon, opaques, carbonate and white mica. Myrmekite is a common feature indicating subsolidus ionic reactions between the feldspar and a fluid phase. The typical grain size of the aplites varies between <0.1 mm and up to about 5 mm, while the pegmatites are coarse-grained with a grain size of up to several cm. The feldspars comprise plagioclase, microcline,

perthite and locally antiperthite, and are, as in the adjacent altered rocks, partly sericitised and replaced by very fine-grained mica and opaque minerals. Quartz contains abundant fluid inclusions. U–Pb-analyses on zircons from a granitoid vein in the quartz syenite of Trollslottet (locality 3) yielded an age of 486 ± 6 Ma, interpreted as the age of magmatic crystallisation (Paulsson, 2003). Titanite formed during alteration of the host rock yielded a U–Pb age of 487 ± 1 Ma (Paulsson, 2003), identical to the age of the granitoid vein.

4. Light alteration zones

4.1. Geometry and width of the alteration zones

The light alteration halos are symmetric on both sides of the central vein and extend with a near-constant width over hundreds of metres. In the homogeneous quartz syenite and charnockite, the boundary between the alteration halos and the unaffected host rock is usually sharp and straight, following the contours of the central vein. In contrast, within the gneisses, the boundaries of the alteration halos appear somewhat less sharp and in places undulating (Fig. 2a and b). At Rakekniven nunatak, two main sets of veins with different orientation are observed (Fig. 2e). Where two or more of these features intersect, the orientation of the veins is irregular and short vein segments with non-uniform thickness appear (Fig. 2f). In places the veins form irregular arrays with a net-like appearance (Fig. 2g). Detailed studies of the mountain faces did not reveal any systematic cross-cutting relations, and a minor offset is only locally observed. These field relations suggest a nearly contemporaneous emplacement within a single geological episode.

The widths of the alteration zones range from decimetres up to several metres. The thickness of the light alteration zone (d_{AZ}) and of the central vein (d_{CV}) was measured directly in the field and estimated on photographs of the nunatak walls where the outcrops were not accessible. For the estimates the error on the absolute widths is large, although probably less than an order of magnitude. However, the d_{AZ}/d_{CV} ratio is not affected by this uncertainty. In principle, it is also independent of the orientation of the vein with respect to a plane outcrop surface. Nevertheless, only veins that appear to make up an angle of more than 60° with the outcrop surface are considered. The mean of 48 d_{AZ}/d_{CV} ratios is about 11 (Fig. 3a). A log d_{AZ} versus log d_{CV} plot shows a linear trend (Fig. 3b), with the slope being in accordance with the typical d_{AZ}/d_{CV} ratio of about 11 (Fig. 3a). There is no marked scale dependence of the d_{AZ}/d_{CV} ratio (Fig. 3c).

4.2. Mineral transformations in the alteration halos

The original high-grade mineral assemblages of the gneiss, charnockite and quartz syenite have undergone

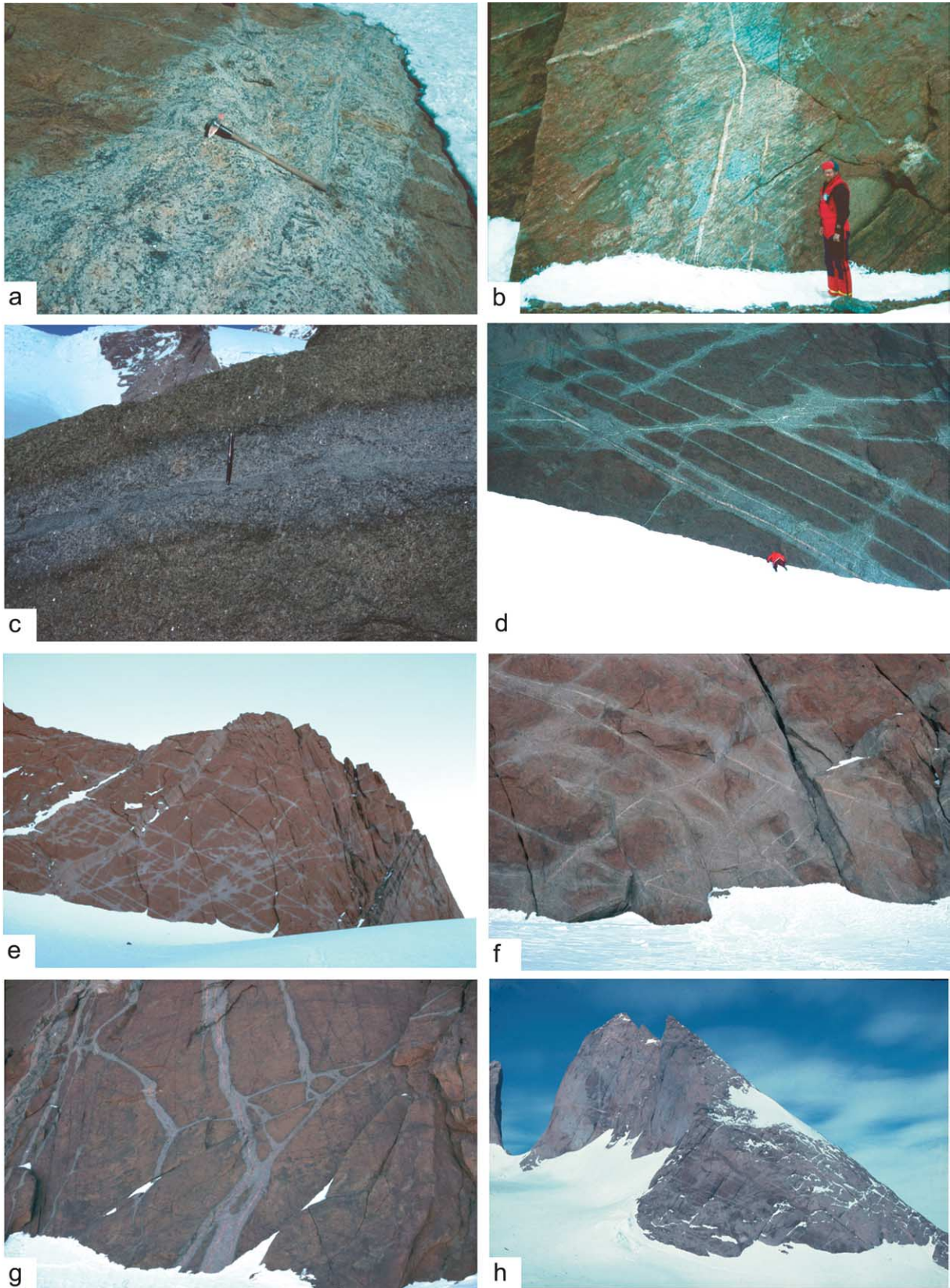


Fig. 2. Photographs showing the field appearance of the light alteration zones and central veins in the nunataks of Mühlig-Hofmann and Filchnerfjella, Dronning Maud Land, Antarctica. (a) Light alteration zone along pegmatite cross-cutting the gneiss of Filchnerfjella (locality 1). (b) Light alteration zone along pegmatite cross-cutting the gneiss of Filchnerfjella. (c) Light alteration zone along aplite cross-cutting the charnockite of Svarthamaren. (d) Light alteration zones along veins cutting the quartz syenite of Rakekniven. The outcrop is about 20 m high (locality 3). (e) Light alteration zones along two sets of veins in

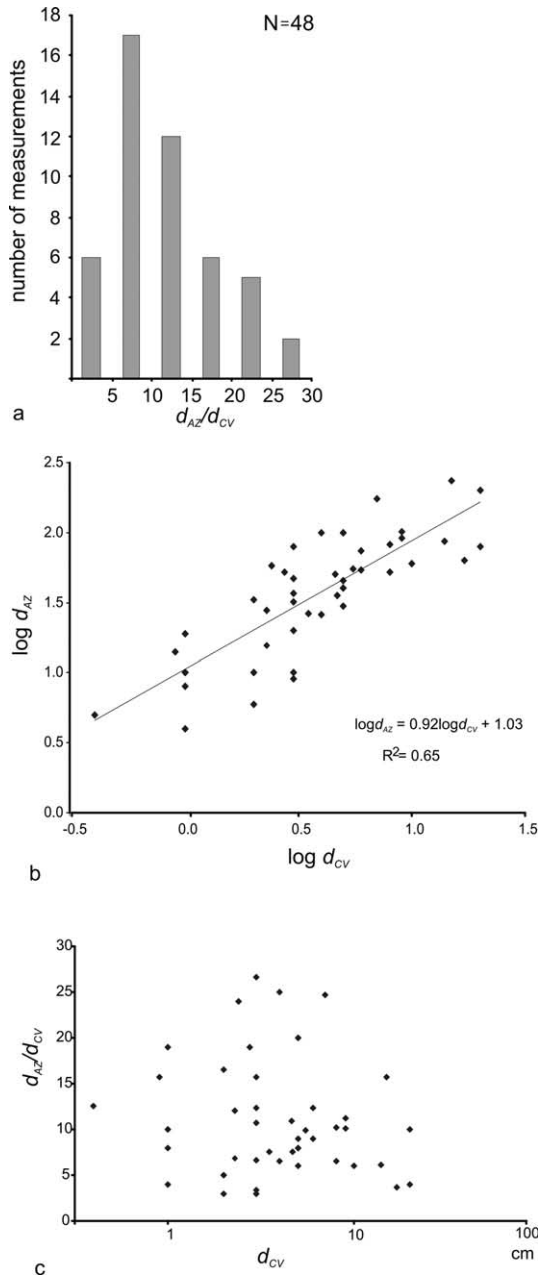


Fig. 3. Relation between the width of the alteration zone (d_{AZ}) and the thickness of the central vein (d_{CV}). The ratio d_{AZ}/d_{CV} is not affected by the uncertainty in absolute length scale (inherent to values determined on photographs of inaccessible outcrop walls) and by the variable inclination of the vein with respect to a flat outcrop surface. (a) Histogram showing the frequency distribution of the observed d_{AZ}/d_{CV} ratios ($N=48$, average 11.3, standard deviation 6.5). (b) Diagram showing the correlation between $\log d_{AZ}$ and $\log d_{CV}$. (c) Diagram showing the ratio d_{AZ}/d_{CV} versus $\log d_{CV}$, with d_{CV} given in cm.

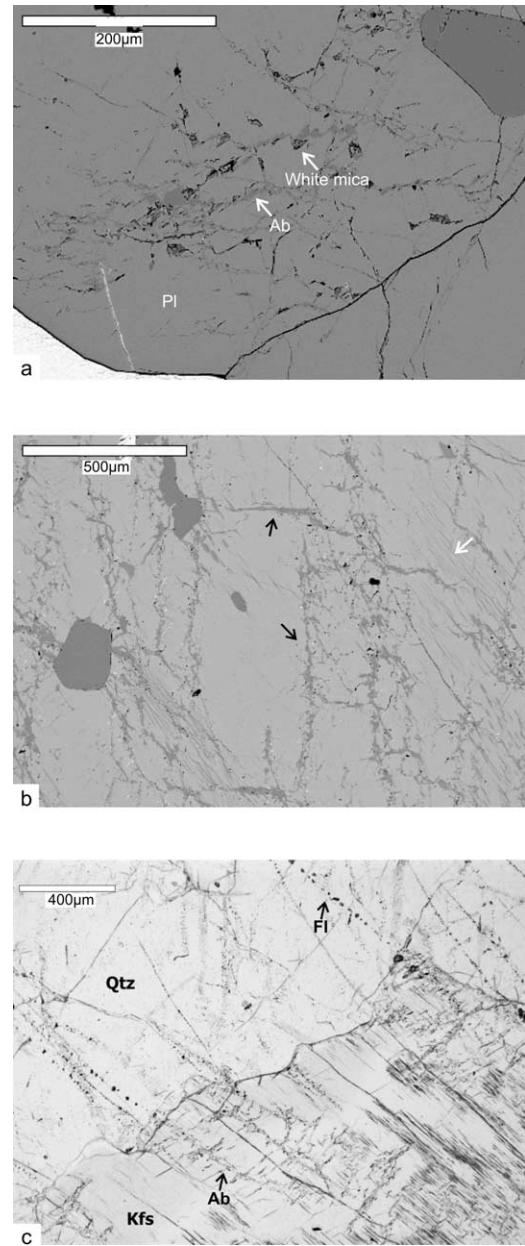
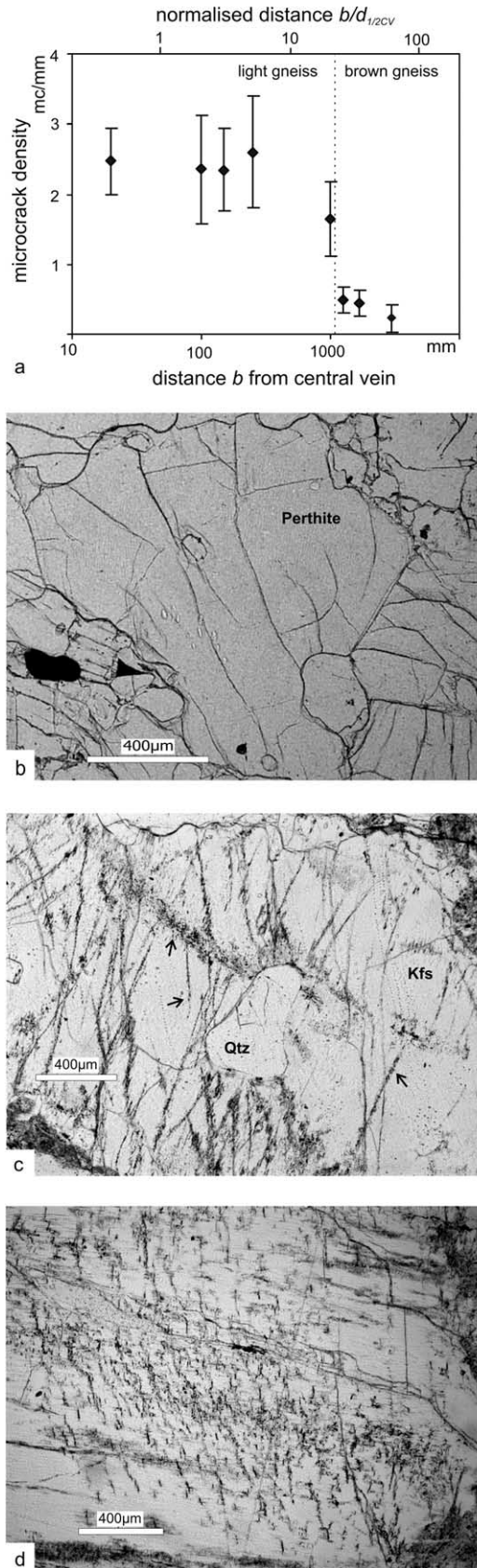


Fig. 4. Microcracks in feldspars and quartz (abbreviations after Kretz (1983)). (a) Plagioclase in altered gneiss transformed to and sealed by albite and mica along irregular microcracks (marked by white arrows; BSE-image, sample AHA205D, $b=15$ cm; $b/d_{1/2CV}=3$). (b) Perthite transected by two sets of irregular microcracks sealed by albite (black arrows) in altered quartz syenite. Relic perthite lamellae are discernible in places (white arrow). In places, the subhorizontal microcracks tend to follow the lamella plane (BSE-image, sample AHA200, $b=20$ cm; $b/d_{1/2CV}=13.3$). (c) Microcrack cutting through grain and interphase boundaries of quartz and K-feldspar in altered charnockite. In quartz the microcracks are healed and discernible by fluid inclusion trails (FI), whereas in feldspar they are sealed by albite (optical micrograph, sample AHA13B).

quartz syenite of Rakekniven. The outcrop is about 300 m high (locality 3). (f) Detail from the outcrop depicted in (e); the shown area is about 15 m high. The width of the light altered-area is increased where two veins intersect. (g) Irregular network of pegmatite veins and related alteration zones in quartz syenite in the wall of Habermehl-toppen. (h) Nunatak in Storskarvet with unaltered brown rock preserved only in small patches. The mountain is about 800 m high.



similar retrogression in the alteration zones. The most conspicuous changes are observed in the feldspars. In thin section, they reveal abundant microcracks (see detailed description below) that cause a partial transformation of perthite to microcline (Figs. 4–6). Plagioclase is replaced by albite and white mica along microcracks (Fig. 4a). Where a high density of microcracks occurs, the transformation has gone to completion (Figs. 5d and 6d). In the vicinity of the microcracks, very fine-grained mica, fluid inclusions and very small grains of opaque minerals are disseminated in the feldspars rendering their dusty or cloudy appearance typical for the altered rocks in the light zones.

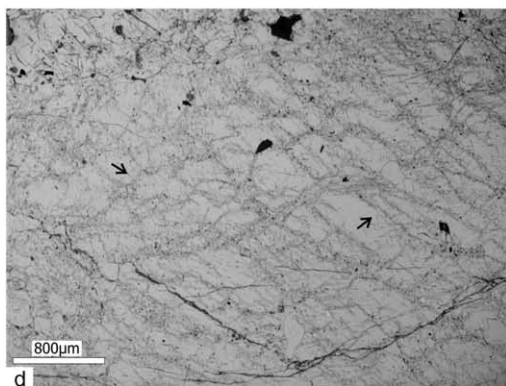
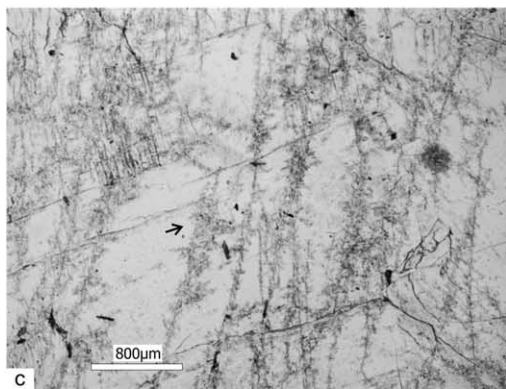
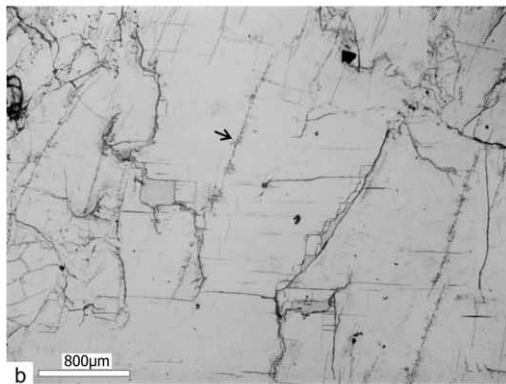
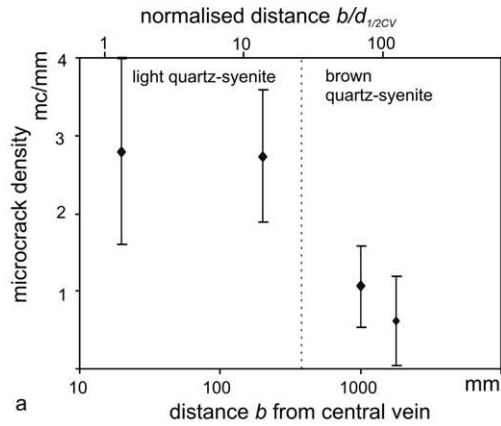
Orthopyroxene is systematically absent in the alteration halos. Instead, symplectites of biotite and quartz are widespread in the altered rocks and are interpreted to have formed at the expense of orthopyroxene. Likewise grunerite, which is present together with orthopyroxene in the quartz syenite, is lacking in the alteration zones. Coarse grains of biotite, hastingsite, plagioclase and quartz are partly replaced by smaller grains. Ilmenite in the original quartz syenite has reacted to form titanite in the altered rock. In the charnockite, small amounts of fine-grained carbonate, chlorite, and green biotite are also formed.

4.3. Microcrack characteristics

The microcracks observed within the alteration zones are healed or sealed, as expected for the given thermal history related to the heat input from the crystallising pegmatitic melts. The term *sealed* is used for microcracks that are filled with minerals different from that of the broken host grain (Fig. 4a and b), while *healed* denotes cracks that were closed by overgrowth on the broken host in crystallographic continuity. In quartz, the microcracks are mainly healed and marked by planar arrays of fluid inclusions. The cracks in feldspar are sealed with albite precipitated from the fluid and decorated with alteration products resulting in a dusty appearance of the feldspars in thin section (Fig. 4c).

The microcracks in the alteration halos are usually plane and transgranular; they cut across grain boundaries and interphase boundaries between different minerals. Commonly one or two distinct sets are observed. Their

Fig. 5. Microcracks distribution and appearance through alteration zone in gneiss (locality 1). (a) Diagram showing the microcrack density, as a function of the distance b from the central vein given in mm, and the dimensionless normalized distance $b/d_{1/2CV}$. Standard deviation given as error bars. (b) Perthite of the brown gneiss showing few and thin microcracks (sample AHA193A, $b=3$ m; $b/d_{1/2CV}=60$). (c) Three sets of microcracks cutting K-feldspar in altered gneiss (arrows). The microcracks show the typical appearance of microcracks formed in the process zone; dusty zones with varying thickness (sample AHA205J, $b=10$ cm; $b/d_{1/2CV}=2$). (d) High density of microcracks in K-feldspar of altered gneiss. With a high density of microcracks, K-feldspar is approaching total transformation (sample AHA205I, $b=2$ cm; $b/d_{1/2CV}=0.4$).



orientation is not controlled by crystallography, except where the orientation of the microcracks approaches that of a cleavage plane. In the quartz syenite the crack length commonly exceeds the diameter of a thin section. The width of the sealed microcracks is up to 50 μm . In the gneiss the crack length appears to be shorter than in the quartz syenite and typically reaches up to 10 mm. Also, in the gneiss many microcracks are more irregular and braiding. Sets of microcracks can be arranged in broader zones up to 1 mm wide (Fig. 5d).

In contrast, the microcracks in the brown unaltered host rocks are mainly intragranular, with typical crack lengths corresponding to grain size. There is no conspicuous alteration of the feldspars related to the cracks.

4.4. Microcrack density as a function of distance from the central vein

The crack density in feldspar is determined by counting the number of microcracks per unit length along transects in thin sections, using samples taken along traverses perpendicular to the veins, similar to the strategy followed by Anders and Wiltschko (1994) and Vermilye and Scholz (1998), for example. As the sealed cracks in feldspars are most conspicuous and unequivocally identified, the density of these microstructural features is determined in the feldspar crystals as a function of distance from the central vein. Note that this partial crack density cannot be taken to represent the original bulk density of microcracks. Unfortunately, as the majority of the samples available have not been oriented in the field, the orientation of the transects cannot be related to the orientation of the central vein. Thus, the crack density is determined along transects with an orientation chosen according to the microstructure of the individual sample: crack density is measured along transects perpendicular and parallel to the trace of the set of the most abundant cracks inclined at a high angle to the section plane. For each gneiss-sample, the density of sealed microcracks in feldspar, given as mc/mm, was determined along 10 transects of 10 mm length. In the quartz syenite, eight transects across feldspar grains with a diameter of about 10 mm from each sample are used. The sealed microcracks were counted using a 4 \times lens, only including features wider than 25 μm . The mean and standard deviation of the measured crack density are displayed in Figs. 5a and 6a as a function of logarithm of the distance b from the central vein,

Fig. 6. Microcrack distribution and appearance through an alteration halo in quartz syenite (locality 3). (a) Diagram showing the microcrack density as a function of distance b from the central vein given in mm, and the dimensionless normalized distance $b/d_{1/2CV}$. (b) Perthite of the brown quartz syenite showing only few microcracks (arrow) (sample AHA197, $b=1.8$ m; $b/d_{1/2CV}=120$). (c) One main set of microcracks cutting K-feldspar in altered quartz syenite (arrow) (sample AHA199, $b=20$ cm; $b/d_{1/2CV}=13.3$). (d) Two sets of microcracks in K-feldspar in altered quartz syenite (arrows); retrogression is almost pervasive (sample AHA200, $b=2$ cm; $b/d_{1/2CV}=1.3$).

and as a function of the dimensionless normalised distance $b/d_{1/2CV}$, which is the ratio between the distance b and the half-width ($d_{CV}/2$) of the vein. The diagrams show that the density of the sealed cracks in feldspar within the light alteration zones is about an order of magnitude higher compared with the unaltered host rock. Within the alteration zones the crack density appears to be constant with about 3 mc/mm, independent of the rock type. The large standard deviation reflects inhomogeneities in crack distribution on the microscale and the contrast in crack density between the two perpendicular directions of the transects.

5. Discussion of structural and petrologic record

5.1. Geometry of the veins and implications for stress field and level of emplacement

Owing to incomplete reactions and widespread disequilibrium in the alteration zone, the level of vein emplacement can hardly be constrained by thermobarometry based on mineral phase equilibria. In view of the K-feldspar in perthite transformed to microcline, sericitisation of plagioclase and newly formed biotite, a broad range of temperatures between about 300 and 500 °C appears feasible (Que and Allen, 1996; Parson and Lee, 2000). Temperatures near 500 °C must have been reached for a short time at the contact with the intruding pegmatitic melt, with a temperature of at least 650 °C, and the hot fluids liberated from the magma upon solidification.

Information on the crustal level can also be achieved from geometric features that reflect brittle failure of the crust. The veins observed in the nunataks of Dronning Maud Land are mostly straight, with approximately plane parallel boundaries, and reveal a high degree of fitting between the opposite walls (Fig. 2), suggesting that the veins formed along brittle tensile cracks. At a deep crustal level brittle failure requires a high pore fluid pressure. For tensile cracks to form by hydraulic fracturing, the pore fluid pressure must exceed the magnitude of the least principal stress by the tensile strength of the rock (e.g. Secor, 1965; Shaw, 1980). The condition for hydraulic fracturing is commonly written as $P_{\text{fluid}} \geq \sigma_3 + T$, with T denoting tensile strength, σ_3 the least principal stress and P_{fluid} the pore fluid pressure. Furthermore, for purely tensile failure to occur, the differential stress $\sigma_1 - \sigma_3$ is restricted to less than about $4T$, based on the form of the Griffith failure envelope (e.g. Shaw, 1980; Suppe, 1985). This strength criterion holds until failure is initiated. When cracks with certain lengths are present, fracture mechanics concepts can be used to describe further crack propagation. For propagation to take place, crack tip stress intensity factors resulting from the prevailing conditions, like stress and temperature, must exceed the fracture toughness of the rock (Boone et al., 1986). It is concluded that the pegmatite veins formed along hydraulic fractures driven by the pressure of the intruding

hydrous melts. In places the veins occur as sets of different orientations without uniform cross-cutting relations, suggesting a nearly contemporaneous timing of the different fracture propagation events. The variable orientation of the veins is taken to indicate that the orientation of the fractures was not controlled by a uniform far-field tectonic stress (as observed for many dike swarms emplaced in the upper crust, e.g. Suppe, 1985), but rather by a local stress field, which can be superimposed on a regional stress field characterised by only low to moderate differential stress. Such low differential stresses are expected for the realm beneath the long-term brittle–ductile transition zone in the continental crust, which means at temperatures above about 300 °C.

The shape of pegmatite bodies as a function of crustal depth, regional stress field and rock anisotropy has been discussed by Brisbin (1986). A tabular shape and preferred orientations are proposed to indicate emplacement along dilatant fractures in the brittle upper crust, while more irregular shapes may reflect emplacement beneath the brittle–ductile transition zone. The shape of the veins and alteration zones of the Mühlig-Hofmann and Filchnerfjella show straight dilatant main fractures with fitting walls (Fig. 2).

Further information is obtained from the fluid inclusions trapped along the healed microcracks (Engvik et al., 2003). The inclusions reveal a fluid composition in the system $\text{H}_2\text{O}-\text{CO}_2$ with a low salinity. Evidence for phase separation during crack healing indicates that the two-phase field in the system $\text{H}_2\text{O}-\text{CO}_2$ was entered during crack healing. For the given low salinity, phase separation during crack healing means cooling to below about 400 °C (Bowers and Helgeson, 1983) within the short time span required for healing. This argument poses an upper bound on the host rock temperatures, which must have been well below 400 °C. Furthermore, the density of the CO_2 -rich inclusions is variable with values between 0.75 and 0.85 g/cm³. The position of the isochores (Shmonov and Shmulovich, 1974) for these densities suggests a trapping pressure of 0.15–0.25 GPa for the presumed temperature range of 300–400 °C.

Based on these considerations it is concluded that the level of emplacement was in the middle crust, near the crustal scale brittle–ductile transition zone at a temperature of about 300–400 °C. For this crustal level and temperature range it is considered very unlikely that the intruding pegmatitic melts followed pre-existing cracks.

5.2. Fluid infiltration causing alteration

The systematic differences between the dark host rock and the material in the alteration halos, as observed in thin sections, indicate that the macroscopic light colour of the altered rocks reflects microstructural changes. The macroscopic effect is suspected to result primarily from the high density of healed and sealed microcracks, and the very high density of interfaces in the fine-grained feldspar alteration

products compared with the coarse-grained host rock. Furthermore, quartz has a milky appearance as it is crowded with secondary fluid inclusions along healed microcracks. Breakdown of the original high-grade mineral assemblages involves hydration and ionic reactions (e.g. Spear, 1993) indicating infiltration of an aqueous fluid from an external source. The infiltration of fluids along microcracks (e.g. Fitz Gerald and Stünitz, 1993) induced mineral reactions combined with a grain size reduction. Paulsson (2003) has found no marked change in composition or oxidation state correlated with the alteration at the locality of Trollsløttest investigated in the present paper.

The composition of fluid inclusions along healed microcracks in the alteration zones show that H₂O and CO₂ are the primary volatile components (Engvik et al., 2003). As the alteration halos developed adjacent to the pegmatitic or aplitic veins, crystallising volatile-rich melts are the likely source of the infiltrating fluids, in accordance with the large grain-size of the pegmatitic veins indicating a volatile-rich melt (e.g. Jahns and Burnham, 1969). The solubility of H₂O in a melt of granitic composition at near-solidus temperatures is about 6 wt.% at 2 kbar and 10 wt.% at 4 kbar (Burnham, 1979). The solubility of CO₂ is much lower, below 1 wt.% for pressures up to 10 kbar (Holloway and Blank, 1994). During cooling and crystallisation of large amounts of feldspar and quartz, with only minor mica and amphibole as OH-bearing minerals, these volatiles need to be liberated as a fluid phase, a process termed second or resurgent boiling (Burnham, 1979). Taking into account the high volatile content of the pegmatitic melt and the low density of an aqueous solution at near-solidus conditions (e.g. Holloway, 1981), the volume of the aqueous solution liberated from the crystallising hydrous magma can be on the same order of magnitude as that of the central pegmatite vein.

5.3. Constraints on the speed of fracture propagation from melt viscosity and thermal considerations

The propagation rate of the magma-driven hydraulic fractures can be constrained as follows: an upper bound on the speed of the fracture propagation can be derived from the viscosity of the volatile-rich melt. The speed of propagation of hydraulic fractures driven by a volatile-rich melt is controlled by the viscosity of the melt (Rubin, 1995). In the present case, the viscosity is not well constrained, as it strongly depends on the concentration of dissolved H₂O (e.g. Lange, 1994; Spera, 1998), which is not precisely known. For instance, the viscosity of a silicic melt can decrease by up to three orders of magnitude when 2 wt.% of H₂O are added (e.g. Lange, 1994, p. 357). This effect becomes less pronounced at higher H₂O concentrations. However, if phase separation has taken place at the top of a magma chamber, fracture propagation could be driven by the segregated fluid phase (Carrington, 1998; Weinberg and Searle, 1999). While the average speed of propagation

would still be controlled by the viscosity of the pegmatitic melt, individual crack propagation events of limited extent could be much faster, and propagation could be jerky. However, in the present study, no discontinuities in the veins and alteration halos were observed that could reflect a jerky propagation on the length scale of an outcrop.

A lower bound on the speed of vein propagation is set by the heat budget of the intruding hydrous melt, and the resulting cooling and solidification rate (e.g. Rubin, 1995). The speed of vein propagation must be sufficient to prevent solidification of the trailing magma column. A slow fracture propagation, as discussed for some joints filled with low temperature alteration products of the host rock (e.g. Segall, 1984a), can thus be ruled out for the propagation of fractures driven by volatile-rich melts at the inferred host rock temperatures of about 300–400 °C.

5.4. Infiltration of fluid into the damaged host rock and lifetime of the highly permeable damage zone

The high density of sealed microcracks in feldspars, and of healed cracks decorated with fluid inclusions in quartz, within the alteration zones (Figs. 4–6), suggest that the transport of fluid from the crystallising hydrous melt into the host rock was controlled by microcracks. The remarkably sharp boundaries of the alteration halos, as shown in Fig. 2, indicate a steep gradient towards a low background permeability of the rocks beyond the zone with the elevated crack density. This is coincidentally reflected by the sharp decline in microcrack density in the feldspars (Figs. 5a and 6a). The alteration is restricted to the zone with high crack densities, subsequently referred to as the damage zone.

Compared with the quartz syenite and charnockite, the boundaries between the alteration zones and the unmodified host rock appear to be more irregular and less sharp in the gneisses. This suggests that the mechanical properties of the host rock, and in particular the marked anisotropy related to the pre-existing foliation of the gneisses, may affect the extent of the damage zone.

The thermal history of the veins and the adjacent host rock can be roughly predicted based on the relations derived by Carslaw and Jaeger (1959). The uncertainty is large, as these relations apply to a stagnant magma and purely conductive heat transport, which both cannot be true in the present case. However, the orders of magnitude in the time scale may be realistic. For a pegmatite sheet of a thickness in the range of decimetres the thermal perturbation may have a life-time of a couple of weeks before the maximum temperature in the centre of the vein has dropped to nearly the pre-intrusive host rock temperature. Experimental studies on healing of microcracks (Smith and Evans, 1984) have revealed that the healing rate is strongly dependent on temperature. At temperatures of 300 °C, healing of microcracks in quartz is predicted to be a matter of days to weeks, and at higher temperatures it may proceed quasi-instantaneously when compared with geological time

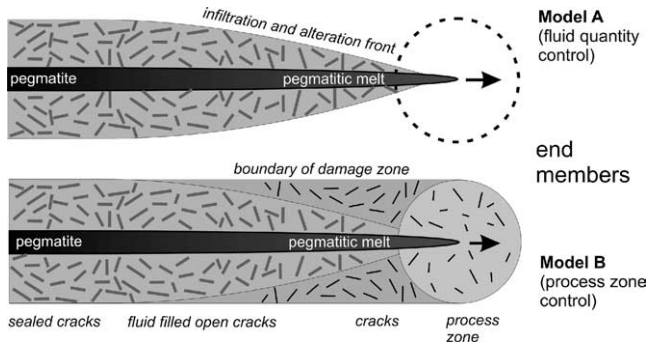


Fig. 7. Alternative hypotheses for the origin of the damage zone. Model (A) assumes crack formation driven by fluids released from the crystallising pegmatitic melt after emplacement, model (B) assumes infiltration of the released fluid into a damage zone created in the process zone at the tip of the propagating main fracture, with the width of the alteration halo already prescribed at that stage.

scales. Therefore it is suspected that the lifetime of the high permeability of the damage zone is very short, and may be even shorter than the time span required for the decay of the thermal perturbation.

6. Origin of the damage zone

6.1. Alternative hypotheses for the origin of the damage zone

The alteration halos along the pegmatitic veins are interpreted to originate from interaction between the host rock and a fluid phase liberated from the pegmatitic melt upon crystallisation. The high density of sealed microcracks within the halos, typically exceeding that of the unaffected host rock by an order of magnitude, indicates that fluid infiltration was controlled by fracture permeability. If so, the width of the conspicuous alteration halo zone reflects the width of the highly permeable fractured zone. In the following, two conceptual end member models for the origin of the fractured and altered zone in the host rock are outlined (Fig. 7):

- (A) Host rock cracking occurs entirely after emplacement of the pegmatitic melt. In this case, hydraulic fractures are driven into the host rock by the fluid phase liberated from the crystallising pegmatitic melt, possibly aided by thermally induced stresses. The width of the alteration halo would then be controlled by the amount of fluid released, hence the quantity of melt, and could therefore correlate with the final width of the central vein.
- (B) Host rock cracking occurs entirely during melt-driven propagation of the main fracture (to become a pegmatite vein later), and the width of the process zone at the propagating tip of the main crack prescribes the width of the alteration halo.

6.2. Evaluation of models (A) and (B)

The merits and shortcomings of the conceptual end member models are discussed below.

Concept (A) appears to be attractive on the first glance in view of the correlation between the width of the central vein and the width of the alteration halo. Intuition suggests that the amount of fluid may control the width of the halo, assuming that the microcracks in the alteration halo originate entirely after emplacement of the batch of pegmatitic melt. In this case, fracturing is supposed to be driven entirely by the fluid liberated from the crystallising pegmatite, possibly facilitated by thermally induced stresses. In model (A), fracturing of the rock in the process zone at the tip of the propagating main crack, driven by the pegmatitic melt, is regarded as irrelevant for the development of the alteration halo. However, model (A) appears to be in conflict with the observed high density of microcracks apparently controlling the width of the halo and the systematic absence of larger hydrothermal veins. The formation of only a few but wider hydraulic fractures would energetically be favourable when created by the released fluid. Also, the sharp boundary between the alteration halo and the unaltered host rock does not support the hydrofracture hypothesis. It would be expected that early-formed cracks would protrude far into the host rock, causing an irregular or lobate shape of the interface. Furthermore, a fracture mechanics analysis on the basis of energetic considerations reveals that the assumed hydraulic fractures, which are necessarily very short compared with the main fracture, would require very large internal pressures to grow. Such high pressures cannot develop in the pegmatitic melt or a released fluid phase as long as the main fracture exists. Thus, appropriate crack driving forces, i.e. stress intensity factor values or strain energy release rates that could have caused the pervasive fragmentation of the host rock in the alteration halo flanking the main fracture, are unrealistic and force us to discard model (A). Instead, the secondary cracks defining the width of the alteration halo must have formed in a highly stressed region, as at the tip of the propagating main fracture, where the stresses are enhanced because of crack tip stress concentration effects.

Concept (B) suggests that the width of the alteration halo recording a transient, high fracture permeability is entirely controlled by the diameter of the process zone at the propagating tip of the main fracture, which is now represented by the pegmatite vein. In this case, the high density of microcracks originates in the process zone and the cracks are subsequently opened or widened by the fluid phase liberated from the crystallising pegmatite. They then act as effective channelways and sites of reaction between fluid and host rock. The retrogression of the host rock is restricted to the damage zone, which has a sharp boundary. We are not aware of a systematic investigation of crack density normal to mode-I tensile fractures in rocks, similar to what has been described for

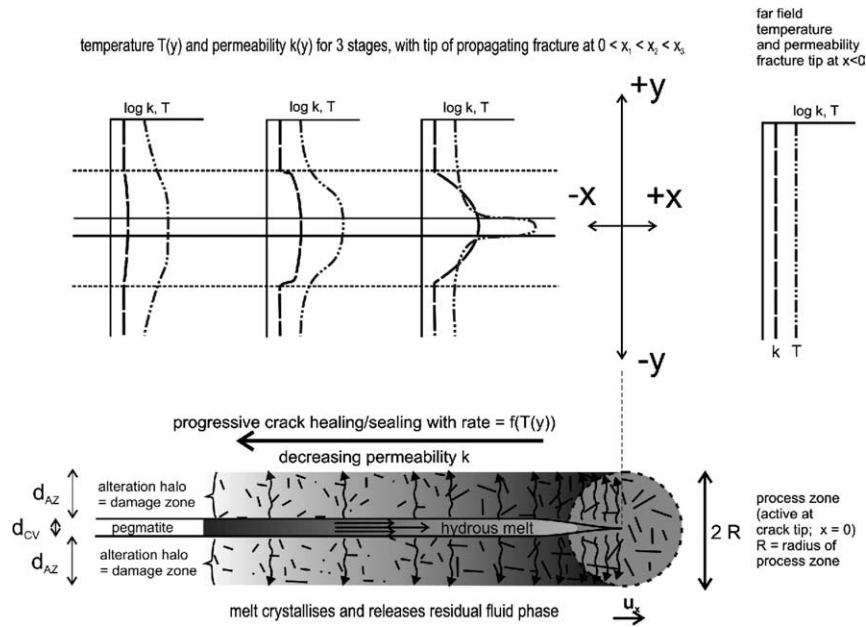


Fig. 8. Preferred conceptual model (see text for discussion).

faults by Vermilye and Scholz (1998), for example. In their study, an exponential decrease of crack density with increasing distance from the fault is observed. There, the width of the damage zone is interpreted to have increased with increasing displacement along the fault. This is different for a dyke originating as a mode-I crack in a single event and lacking subsequent displacement parallel to the fracture. The observed pattern of crack density and the sharp boundary of the damage zone thus may not necessarily be in conflict with the crack densities observed by Vermilye and Scholz (1998) at a fault. In the case of the pegmatite veins, the damage is supposed to originate in the process zone during the short stage when the tip of the fracture passes by, and a later modification of the width of the damage zone can be excluded.

While hypothesis (A) appears to be in conflict with energetic considerations and geometrical aspects, hypothesis (B) poses no major conflicts and is thus taken to represent a suitable conceptual scenario to explain the constant width and sharp boundaries of the alteration halos

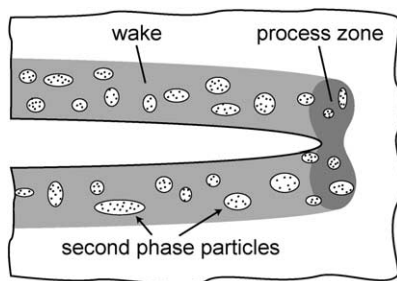


Fig. 9. Schematic of the process zone (dog bone model) in ceramics with second phase particles and the wake of damage trailing the advancing crack tip (after Anderson, 1991).

along the pegmatite veins. Some conceptual aspects of model (B) are detailed in Fig. 8, and a mechanical model is presented in the subsequent chapter.

6.3. Process zone and damage zone in rock deformation

A process zone with inelastic deformation develops around the propagating tip of the macroscopic fracture during faulting and dyke propagation (Atkinson, 1987; Rubin, 1993; Scholz et al., 1993; Anders and Wiltchko, 1994; Vermilye and Scholz, 1998; Scholz, 2002). Within the process zone, local failure by both crystal plastic deformation and microcracking may occur concomitantly, driven by the high stress concentration. The advancing process zone at a tip of a propagating crack leaves a wake with damaged zones to both sides of the fracture surface behind, the width of this wake being controlled by the size of the process zone. Such processes were also observed in ceramics with second phase particles, resulting in non-linear deformations at the crack tip (Fig. 9; Anderson, 1991). In laboratory experiments, the formation of microcracks in the process zone can be monitored by analysis of acoustic emissions (e.g. Lockner, 1995; Zang et al., 2000) and afterwards compared with the microstructure of the deformed sample (e.g. Swanson, 1987; Janssen et al., 2001).

The crack density is a characteristic property of the damage zone and has been investigated at natural faults by Anders and Wiltchko (1994) and Vermilye and Scholz (1998), for example. Anders and Wiltchko (1994) concluded from their data that the width of the damage zone does not significantly depend on the displacement along the fault, while other authors (e.g. Vermilye and Scholz, 1998; Lyakhovsky, 2001; Scholz, 2002) report such a dependency.

The damage zone is proposed to exhibit a high permeability and therefore to contribute significantly to the bulk transport properties of faults (Vermilye and Scholz, 1998; Scholz, 2002).

Compared with the studies on the damage zone along faults, less attention has so far been paid to the damage zone along veins and dykes, which are supposed to originate as mode-I fractures (e.g. Rubin, 1995). An experimental study based on acoustic emissions from propagating hydraulic mode-I fractures in Weber Sandstone was carried out by Lockner and Byerlee (1977). An ongoing laboratory scale study on tensile fracturing of granite using acoustic emissions (G. Dresen, personal communication, 2003) shows a process zone similar in extent to that observed by Zang et al. (2000) for shear fractures, within the limits of spatial resolution.

The damage zone along magmatic veins and dykes in nature may be poorly preserved due to extensive annealing caused by magmatic heat input. In the present study, the lateral extent of the damage zone is obviously reflected by the conspicuous light alteration zones. However, the original type of damage created during propagation of the main fracture has probably undergone significant modification during subsequent contact metamorphism and infiltration of hot fluid. In contrast to the case studies on faults in the upper crust (Anders and Wiltschko, 1994; Vermilye and Scholz, 1998), the thermal history of the host rock adjacent to the magmatic veins must have favoured crack healing and possibly obliterated a considerable part of the original imprint. Thus, the crack densities determined for the feldspars and their variation as a function of the distance from the centre of the veins cannot be directly compared with the results obtained for faults in the upper crust (Scholz, 2002) or in laboratory experiments.

Furthermore, in contrast to the damage zones developing along faults, the damage zones along magmatic dykes probably develop during the short stage of fracture propagation. Therefore, the alteration zones dealt with in the present study possibly reflect the diameter of the process zone at the tip of the propagating mode-I fracture, without subsequent modification by successive increments of fracture-parallel shear, as in the case of faults. The width of the alteration zone scales with the width of the central vein. This implies that the width of the damage zone reflects the radius of the process zone and, additionally, that the final width of the propagating hydraulic fracture (the pegmatite vein) is already determined at the stage of crack propagation. In this case the final width of the vein is determined by a specific property or condition, e.g. the excess pressure of the intruding magma or the speed of fracture propagation that also controls the radius of the process zone. As the rate of propagation of a dyke depends on $(d_{1/2CV})^2$, a thicker vein representing a wider and longer magma-filled fissure behind the propagating tip of the fracture may have allowed a faster propagation (Rubin, 1995). A fracture mechanics based consideration describing these dependencies is given in a

subsequent chapter. Rubin (1993) has discussed the dependence of the diameter of the process zone on the length of a dyke. In the present case, it is not clear how the width of the veins scales with their length, as the latter exceeds the typical length scale of the outcrops.

Thus, the final thickness of the vein cannot be a result of successive inflation, which appears feasible in view of the restricted heat content of the pegmatitic magma, the thickness of the veins, and the significantly lower temperature of the host rock. A thicker vein will cool more slowly and produce a wider contact aureole, with higher temperatures and more time for crack healing and sealing at any distance from the contact.

6.4. A qualitative model for the formation of the alteration zones

Based on the considerations outlined above, Fig. 8 presents a qualitative synoptic scheme visualizing the envisaged combination of processes responsible for the formation of the light alteration halos flanking the aplitic to pegmatitic veins in Dronning Maud Land. The scheme is partly based on a figure drawn for a propagating dyke in Rubin (1995), and complemented to show the process zone (assumed to be circular in two dimensions following Irwin's model of the process zone, waisted according to the more realistic dog bone model used in Fig. 9) and the trailing wake as the resulting final damage zone. Symbols are used to visualise the infiltrating fluid and the progressive decrease of permeability due to crack healing and sealing. The time scale of the visualised sequence of process is bracketed by the speed of propagation of the hydraulic fracture controlled by the viscosity of the volatile-rich melt and the rate of cooling and solidification of the magma (Rubin, 1995). The significance of the diameter of the process zone is discussed in the subsequent chapter.

7. A mechanical model for the development of the damage zone and some implications

Accepting the general validity of concept (B), and assuming that the process zone at the tip of the main fracture with damage by irreversible microcrack formation can be treated in analogy to the fracture mechanics concept of small scale yielding developed for metallic materials (e.g. fracture mechanics textbooks by Broek (1987), Anderson (1991) and Broberg (1999)), the width of the crack tip process zone—based on model considerations by Irwin—correlates with the stress intensity factor prevailing at the crack tip according to the relationship for plane strain conditions:

$$r_{pz} = \frac{1}{2\pi} \left(\frac{K_I}{1.68\sigma_{US}} \right)^2 \quad (1)$$

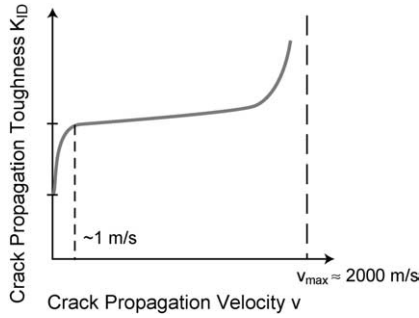


Fig. 10. Dependence of fracture toughness of rocks on crack propagation velocity, showing a sharp increase of fracture toughness at low velocities.

where r_{pz} = radius of the process zone, K_I = mode-I stress intensity factor, and σ_{US} = ultimate tensile strength of the material for microcrack formation. Since the main fracture is expanding in length, the stress intensity factor K_I of the propagating crack is equal to (or larger than) the crack propagation toughness K_{ID} of the material for the specific velocity v_{prop} of crack propagation, with $K_I = K_{ID}(v = v_{prop})$. The fracture toughness K_{ID} of propagating cracks in rocks as a function of crack propagation velocity $K_{ID}(v)$ is typically given by a dependence as shown in Fig. 10 (Bertram and Kalthoff, 2003). It should be noted that—for velocities in the range of metres per second, i.e. the velocities of interest in the present context—small velocity changes cause large changes in fracture toughness and, consequently, cause large changes in the diameter of the process zone.

The concept implies that the crack propagation velocity of the main fracture is constant and equal to the velocity of the injection of the viscous pegmatitic melt, which is estimated to be in the range of a few m/s. Based on this assumption, the fracture toughness of the rock has a certain value for the ambient conditions. For this fracture toughness value, which applies for the propagating main fracture, the diameter of the process zone at its tip has a constant value independent of the actual crack length.

For the crack, loaded along the crack surfaces by an internal pressure P_0 of the intruding pegmatitic melt, the stress intensity factor increases with crack length a according to a square root of crack length relationship, given as:

$$K_I = P_0 \sqrt{\pi a} \quad (2)$$

Assuming that the pressure of the pegmatitic melt would be constant, the stress intensity factor K_I would increase with increasing crack length. Consequently, for very long crack lengths—as observed in the present case— K_I would reach unrealistic values. According to the underlying model, the actual stress intensity factor at the tip of a propagating crack equals the specific fracture toughness of the material for the given crack propagation velocity and, therefore, must be constant. This leads to the conclusion that the pressure P_0 of the pegmatitic melt at distances further away from the crack tip must have been reduced and that the distant realms

(with respect to the tip of the main fracture) of the crack surfaces do not contribute significantly to the stress intensity factor anymore. With this consideration, the overall stress intensity factor K for the advancing main fracture assumes a constant value that is equal to the specific fracture toughness K_{ID} of the rock.

The model of a crack with a process zone at its tip, where microcracks form under the influence of the enhanced stress field, results in a permanent displacement of the fracture surfaces (crack opening width). As a first order consideration this is given by the opening displacement 2δ of the underlying crack model after Irwin at a distance r_{trans} behind the crack tip, with the distance r_{trans} specified by the transition line of undamaged material to material weakened by irreversible damage processes. With the general expression for the opening displacement 2δ of the crack surfaces given in dependence of the radial distance r behind the crack tip (for plane strain conditions):

$$2\delta = \frac{8(1 - \nu^2)}{E} K_I \sqrt{\frac{r}{2\pi}} \quad (3)$$

and, furthermore, the borderline between undamaged and damaged material in the process zone given by the radius of the Irwin crack tip process zone, the remaining crack width—in analogy to the crack tip opening displacement as defined in conventional small scale yielding fracture mechanics concepts for metallic materials—is given as:

$$CTOD = 2\delta \Big|_{trans} = \frac{8(1 - \nu^2)}{\pi E} \frac{K_I^2}{1.68\sigma_{US}} \quad (4)$$

Eqs. (1) and (4) result in a fixed relationship between the size of the process zone (with r_{pz} being equivalent to the width of the alteration zone d_{AZ}) and the displacement of the crack surfaces (with CTOD being equivalent to the width of the central vein d_{CV}) of the main fracture (Fig. 11). Such a relationship between d_{AZ} and d_{CV} is observed for the pegmatite veins and their alteration halos. Using rough estimates for the Young's modulus E , the Poisson ratio ν , and the ultimate tensile strength σ_{US} , with $E = 5\text{--}50$ GPa, $\sigma_{US} = 5\text{--}50$ MPa, and $\nu = 0.3$, a ratio $r_{pz}/CTOD$ ranging from 4 to 400 results. This compares with the observed d_{AZ}/d_{CV} ratio of about 11.

For one specific fracture event with fixed environmental conditions of the rock, i.e. temperature and confining pressure, the applying fracture toughness value specifies a diameter of the process zone, i.e. the alteration zone (d_{AZ})

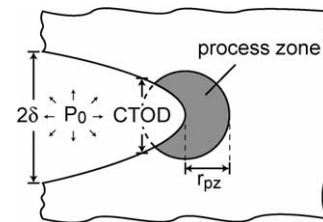


Fig. 11. Irwin model of the crack tip opening displacement.

and a width of the vein (d_{CV}) being practically constant for the whole event. Other diameters of the process zone and the correlated width of the vein would result for other fracture events under different environmental conditions. Small variations of the size of the process zone and the correlated width of the vein (see Section 6.3; Rubin, 1995) observed in one fracture event are explained by small variations of the crack propagation velocity, which accordingly result in somewhat different values of the crack propagation fracture toughness. These interdependent relationships are supported by observations made by Segall (1984b). The author shows a photograph of a vein and alteration halo for a crack that apparently has slowed down and finally come to arrest, resulting in a continuously decreasing size of both the width of the alteration zone and the width of the vein itself. Furthermore, in laboratory acoustic emission measurements, Swanson (1984) found that the activity in the process zone occurred closer to the crack surfaces and at lower rates when the crack speed was reduced.

8. Conclusions

The unique outcrops of Dronning Maud Land yield insight into magma-driven hydraulic fracturing and the origin of alteration halos. The pegmatitic veins are interpreted to represent mode-I hydraulic fractures driven by a volatile-rich melt with a minimum temperature of 650 °C, emplaced in the middle crust near the brittle–ductile transition zone with a far field host rock temperature of 300–400 °C. The conspicuous alteration halos flanking the veins reflect the extent of microcrack-controlled infiltration of the fluid phase liberated from the crystallising pegmatitic melt into the damaged high grade metamorphic host rock. The following points are emphasized:

- (1) The correlation between the density of sealed microcracks in feldspar, the degree of retrogression of the originally high-grade metamorphic host rock, and the lateral extent of the light alteration zones with sharp boundaries indicates that fluid infiltration and related retrogression of the host rocks was controlled by the transient high permeability of the damage zone formed by the wake of the process zone at the tip of the propagating main fracture.
- (2) In contrast to faults, the propagation of the central fracture and emplacement of the pegmatite took place in a single event. It is proposed that the width of the damage zone corresponds to the radius of the process zone at the tip of the propagating hydraulic fracture, and—in contrast to the situation at faults—may not be subject to later modification. Mechanical considerations suggest that the width of the damage zone scales with the crack propagation toughness of the growing main fracture, which in turn is controlled by the speed of crack propagation. Furthermore, the width of the

damage zone—according to the model—is correlated with the thickness of the resultant vein.

- (3) Finally, it is proposed that the infiltration and retrogression of the high-grade rocks in the damage zone was a quasi-instantaneous process on a geological time scale, as healing of microcracks is expected to be very fast at $T > 300$ °C. Therefore the host-rock permeability created during propagation of the main fracture must have been short-lived (days to weeks).

Whether the concept holds true for the widespread alteration halos along joints and fissures in general remains to be explored. The excellent exposure of the phenomenon in Dronning Maud Land provides an idea of how short-term fracture-controlled fluid infiltration and related retrogression can affect extensive crustal volumes. The high volume percentage of the light alteration zones observed throughout the mountain range over hundreds of kilometres, independent of lithological variations and with occasionally entire nunataks being altered, shows that such fracture-controlled short-term fluid infiltration processes can be effective on a regional scale in the middle crust. It is suspected that the role of such processes is generally underestimated being inconspicuous in areas with less favourable exposure and weathering.

Acknowledgements

Fieldwork for this study was carried out during the Norwegian Antarctic Research Expedition 1996/97 and was financed by the Norwegian Polar Institute and the Norwegian Research Council (NFR). We are thankful to our field partner, O. Paulsson, for his contribution to the fieldwork, discussions and company during our stay in Antarctica. Additional funding from NFR (145569/432 to A.K.E.) and from the German Science Foundation within the scope of Collaborative Research Center 526 “Rheology of the Earth” at Ruhr-University Bochum is gratefully acknowledged. We also gratefully acknowledge helpful comments and suggestions by Paul Bons and Sandra Piazzolo, and careful reviews by Yves Leroy and an anonymous referee.

References

- Anders, M.H., Wiltschko, D.V., 1994. Microfracturing, paleostress and the growth of faults. *Journal of Structural Geology* 16, 795–815.
- Anderson, T.L., 1991. *Fracture Mechanics: Fundamentals and Application*. CRC Press, Boca Raton.
- Atkinson, B.K., 1987. Introduction to fracture mechanics and its geophysical applications. In: Atkinson, B.K. (Ed.), *Fracture Mechanics of Rocks*. Academic Press, London, pp. 1–26.
- Austrheim, H., 1990. The granulite–eclogite facies transition: a comparison of experimental work and natural occurrence in the Bergen Arcs, western Norway. *Lithos* 25, 163–169.
- Bertram, A., Kalthoff, J.F., 2003. Crack propagation toughness of rock for

- the range from low to very high crack speeds. In: Buchholz, F.-G., Richard, H.A., Aliabadi, M.H. (Eds.), *Advances in Fracture and Damage Mechanics Key Engineering Materials*, 251–252. Trans Tech Publications, Uetikon-Zurich, pp. 423–430.
- Boone, T.J., Wawrzynek, P.A., Ingraffea, A.R., 1986. Simulation of the fracture process in rock with application to hydrofracturing. *International Journal of Rock Mechanics and Mining Sciences* 23/3, 255–265.
- Bowers, T.S., Helgeson, H.C., 1983. Calculation of the thermodynamic and geochemical consequences of nonideal mixing in the system $\text{H}_2\text{O}-\text{CO}_2-\text{NaCl}$ on phase relations in geological systems: equation of state for $\text{H}_2\text{O}-\text{CO}_2-\text{NaCl}$ fluids at high pressure and temperatures. *Geochimica and Cosmochimica Acta* 47, 1247–1275.
- Brisbin, W.C., 1986. Mechanics of pegmatite intrusion. *American Mineralogist* 71, 644–651.
- Broek, D., 1987. *Elementary Engineering Fracture Mechanics*, 4th ed Martinus Nijhoff Publishers, Dordrecht.
- Broberg, K.B., 1999. *Cracks and Fracture*. Academic Press, San Diego.
- Burnham, C.W., 1979. The importance of volatile constituents. In: Yoder, H.S. (Ed.), *The Evolution of the Igneous Rocks*. Princeton University Press, pp. 439–482.
- Carrington, C.R., 1998. Plumbing systems. In: Sigurdsson, H. (Ed.), *Encyclopedia of Volcanoes*. Academic Press, pp. 219–235.
- Carslaw, H.S., Jaeger, J.C., 1959. *Conduction of Heat in Solids*, 2nd ed Oxford and the Clarendon Press, London.
- Cox, K.G., Bell, J.D., Pankhurst, R.J., 1979. *The Interpretation of Igneous Rocks*. George Allen & Unwin, London.
- Elworthy, T.P., 1982. Geochronology. In: Wolmarans, L.G., Kent, L.E. (Eds.), *Geological Investigations in Western Dronning Maud Land, Antarctica: a Synthesis South African Antarctic Research Supplement*, 2, pp. 73–83.
- Engvik, A.K., Elvevold, S., 2004. Pan-African extension and near-isothermal exhumation of a granulite facies terrain, Dronning Maud Land, Antarctica. *Geological Magazine* 141–6, 1–12.
- Engvik, A.K., Austrheim, H., Stöckert, B., Elvevold, S., 2003. Magma-driven hydraulic fracturing and infiltration of $\text{CO}_2-\text{H}_2\text{O}$ fluids into high-grade crystalline rocks, Dronning Maud Land, Antarctica. *Terra Nostra* 4, 82–83. Abstracts.
- Fitz Gerald, J.D., Stünitz, H., 1993. Deformation of granitoids at low metamorphic grade. I: reactions and grain size reduction. *Tectonophysics* 221, 269–297.
- Fitzsimons, I.C.W., 2000. A review of tectonic events in the East Antarctic Shield and their implications for Gondwana and earlier supercontinents. *Journal of African Earth Sciences* 31, 3–23.
- Holloway, J.R., 1981. Composition and volume of supercritical fluids in the earth's crust. In: Hollister, L.S., Crawford, M.L. (Eds.), *Short Course In Fluid Inclusions: Applications to Petrology*. Mineralogical Association of Canada, Calgary, pp. 13–38.
- Holloway, J.R., Blank, J.G., 1994. Application of experimental results to C–O–H species in natural melts. In: Carroll, M.R., Holloway, J.R. (Eds.), *Volatiles in Magma Reviews in Mineralogy*, 30, pp. 331–370.
- Huang, W.L., Wyllie, P.J., 1981. Phase relationships of S-type granite with H_2O to 35 kbar: muscovite from Harney Peak, South Dakota. *Journal of Geophysical Research* 86, 10515–10529.
- Jacobs, J., Fanning, C.M., Henjes-Kunst, F., Olesch, M., Paech, H.-J., 1998. Continuation of the Mozambique Belt into East Antarctica: Grenville-age metamorphism and polyphase Pan-African high-grade events in Central Dronning Maud Land. *Journal of Geology* 106, 385–406.
- Jahns, R.H., Burnham, C.W., 1969. Experimental studies of pegmatite genesis: I. A model for the derivation and crystallization of granitic pegmatites. *Economic Geology* 64, 843–864.
- Janssen, C., Wagner, F.C., Zang, A., Dresen, G., 2001. Fracture process zone in granite: a microstructural analysis. *International Journal of Earth Sciences* 90, 46–59.
- Kostenko, O., Jamtveit, B., Austrheim, H., Pollok, K., Putnis, C., 2002. The mechanism of fluid infiltration in peridotites at Almklovdaalen, western Norway. *Geofluids* 2, 203–215.
- Kretz, R., 1983. Symbols for rock-forming minerals. *American Mineralogist* 68, 277–279.
- Lange, R.A., 1994. The effect of H_2O , CO_2 , and F on the density and viscosity of silicate melts. In: Carroll, M.R., Holloway, J.R. (Eds.), *Volatiles in Magma Reviews in Mineralogy*, 30, pp. 331–370.
- Lockner, D.A., 1995. Rock failure. In: Ahrens, T.J. (Ed.), *Rock Physics and Phase Relations—a Handbook of Physical Constants*. American Geophysical Union, Washington, pp. 127–147.
- Lockner, D.A., Byerlee, J.D., 1977. Hydrofracture in Weber sandstone at high confining pressure and differential stress. *Journal of Geophysical Research* 82, 2018–2026.
- Lyakhovskiy, V., 2001. Scaling of fracture length and distributed damage. *Geophysical Journal International* 144, 114–122.
- Markl, G., Piazzolo, S., 1998. Halogen-bearing minerals in syenites and high-grade marbles of Dronning Maud Land, Antarctica: monitors of fluid compositional changes during late-magmatic fluid–rock interaction processes. *Contributions to Mineralogy and Petrology* 132, 246–268.
- Merrill, R.B., Robertson, J.K., Wyllie, P.J., 1970. Melting reactions in the system $\text{NaAlSi}_3\text{O}_8-\text{KAlSi}_3\text{O}_8-\text{SiO}_2-\text{H}_2\text{O}$ at 20 kbars compared with results for other feldspar–quartz– H_2O and rock– H_2O systems. *Journal of Geology* 78, 558–569.
- Mikhalsky, E.V., Beliatsky, E.V., Savva, E.V., Wetzel, H.-U., Federov, L.V., Weiser, Th., Hahne, K., 1997. Reconnaissance geochronologic data on polymetamorphic and igneous rocks of the Humboldt Mountains, Central Queen Maud Land, East Antarctica. In: Ricci, C.A. (Ed.), *The Antarctic Region: Geological Evolution and Processes*. Terra Antarctica Publications, Siena, pp. 45–53.
- Moyes, A.B., 1993. The age and origin of the Jutulsessen granitic gneiss, Gjelsvikfjella, Dronning Maud Land. *South African Journal of Antarctic Research* 23, 25–32.
- Ohta, Y., 1999. Nature Environment map, Gjelsvikfjella and Western Mühlig-Hofmannfjella, sheets 1 and 2, Dronning Maud Land. Norwegian Polar Institute, Temakart nr. 24.
- Ohta, Y., Tørrudbakken, B., Shiraishi, K., 1990. Geology of Gjelsvikfjella and Western Mühlig-Hofmannfjella, western Dronning Maud Land, East Antarctica. *Polar Research* 8, 99–126.
- Parson, I., Lee, M.R., 2000. Alkali feldspars as microtextural markers of fluid flow. In: Stober, I., Bucher, K. (Eds.), *Hydrogeology of Crystalline Rocks*. Kluwer Academic Publishers, pp. 27–50.
- Paulsson, O., 2003. U–Pb geochronology of tectonothermal events related to the Rodinia and Gondwana supercontinents—observations from Antarctica and Baltica. *Litholund theses* 2, Lund University, Sweden.
- Que, M., Allen, A.R., 1996. Sericitization of plagioclase in Rosses Granite Complex, Co. Donegal, Ireland. *Mineralogical Magazine* 60, 927–939.
- Rubin, A.M., 1993. Tensile fracture of rock at high confining pressure: implications for dike propagation. *Journal of Geophysical Research* 98, 15919–15935.
- Rubin, A.M., 1995. Propagation of magma filled cracks. *Annual Review of Earth and Planetary Science* 8, 287–336.
- Scholz, C.H., 2002. *The Mechanics of Earthquakes and Faulting*, 2nd ed Cambridge University Press, Cambridge.
- Scholz, C.H., Dawers, N.H., Yu, J.-Z., Anders, M.H., Cowie, P.A., 1993. Fault growth and fault scaling laws: preliminary results. *Journal of Geophysical Research* 98, 21951–21961.
- Secor, D.T., 1965. Role of fluid pressure in jointing. *American Journal of Science* 263, 633–646.
- Segall, P., 1984a. Rate-dependent extensional deformation resulting from crack growth in rocks. *Journal of Geophysical Research* 89, 4185–4195.
- Segall, P., 1984b. Formation and growth of extensional fracture sets. *Geological Society of America, Bulletin* 95, 454–462.
- Segall, P., Pollard, D.D., 1983. Joint formation in granitic rock of the Sierra Nevada. *Geological Society of America, Bulletin* 94, 563–575.
- Shaw, H.R., 1980. The fracture mechanism of magma transport from the mantle to the surface. In: Hargraves, R.B. (Ed.), *Physics of Magmatic Processes*. Princeton University Press, Princeton.
- Shmonov, V.M., Shmulovich, K.I., 1974. Molar volumes and equation of

- state of CO₂ at temperatures from 100 to 1000 °C and pressures from 2000 to 10,000 bars. *Transactions (Doklady) of the U.S.S.R. Academy of Sciences: Earth Science Sections* 217, 206–209.
- Smith, D.L., Evans, B., 1984. Diffusional crack healing in quartz. *Journal of Geophysical Research* 89, 4125–4135.
- Spear, F.S., 1993. *Metamorphic Phase Equilibria and Pressure-Temperature-Time Paths*. Mineralogical Society of America (Monograph), Washington.
- Spera, F.J., 1998. Physical properties of magma. In: Sigurdsson, H. (Ed.), *Encyclopedia of Volcanoes*. Academic Press, pp. 171–190.
- Suppe, J., 1985. *Principles of Structural Geology*. Prentice-Hall, Englewood Cliffs, New Jersey.
- Swanson, P.L., 1984. Subcritical crack growth and other time- and environment-dependent behavior in crustal rocks. *Journal of Geophysical Research* 89/B6, 4137–4152.
- Swanson, P.L., 1987. Tensile fracture resistance mechanisms in brittle polycrystals: an ultrasonics and in situ microscopy investigation. *Journal of Geophysical Research* 92/B8, 8015–8036.
- Vermilye, J.M., Scholz, C.H., 1998. The process zone: a microstructural view of fault growth. *Journal of Geophysical Research* 103, 12223–12237.
- Weinberg, R.F., Searle, M.P., 1999. Volatile-assisted intrusion and autometasomatism of leucogranites in the Khumbu Himalaya, Nepal. *Journal of Geology* 107, 27–48.
- Zang, A., Wagner, C.F., Stanchits, S., Janssen, C., Dresen, G., 2000. Fracture process zone in granite. *Journal of Geophysical Research* 105, 23651–23661.